Carbon–Nitrogen Cleavage and Carbon–Carbon Coupling Processes in the Reactions of $Ru_3(CO)_{12}$ with Tertiary Amines

Michael Day, Sharad Hajela, Kenneth I. Hardcastle, Tim McPhillips, and Edward Rosenberg*

Department of Chemistry, California State University, Northridge, California 91330

Mauro Botta, Roberto Gobetto, Luciano Milone,* and Domenico Osella

Dipartimento di Chimica Inorganica, Chimica Fisica e Chimica dei Materiali, Università di Torino, Via Giuria 7-9, I 10125 Torino, Italy

Robert W. Gellert

Department of Chemistry, California State University, Los Angeles, California 90024

Received May 11, 1989

The reactions of triethylamine and ethyldiisopropylamine with $Ru_3(CO)_{12}$ promoted by $Fe_2(CO)_4(P(C_6H_5)_3)_2(\mu\text{-}SCH_2CH_3)_2$ at 70 °C have been studied. In addition to the previously reported major product $(\mu\text{-}H)(\mu_3\text{-}\eta^2\text{-}CH_3C{=}NCH_2CH_3)Ru_3(CO)_9$ (**1**), the three other triruthenium products formed, $(\mu\text{-}H)(\mu_3\text{-}\eta^3\text{-}CH_2CH{=}NCH_2CH_3)Ru_3(CO)_9$ (**2**), $(\mu\text{-}H)(\mu_3\text{-}\eta^3\text{-}CH_3CC(H)C{=}N(CH_2CH_3)_2)Ru_3(CO)_9$ (**3**), and $(\mu\text{-}H)(\mu_3\text{-}\eta^3\text{-}(CH_3CH_2)_2N{=}C(H)C(H)CCH_2)Ru_3(CO)_9$ (**4**), have been characterized by spectroscopic methods and in the case of **3** and **4** by solid-state structural investigations. Compounds **1** and **2** are structural isomers, both of which have undergone alkyl cleavage, while **3** and **4** result from C–C coupling of a C_2 fragment to a $(C_2H_4)N(CH_2CH_3)_2$ fragment. In the reaction of the bulkier ethyldiisopropylamine under the same conditions as above, only two triruthenium–amine products are formed, $(\mu\text{-}H)_2(\mu_3\text{-}\eta^2\text{-}HCC{=}N(CH(CH_3)_2)_2Ru_3(CO)_9$ (**5**) and $(\mu\text{-}H)(\mu_3\text{-}\eta^2\text{-}CC{=}N(CH(CH_3)_2)_2Ru_3(CO)_9$ (**6**), which were characterized by solid-state structural investigations and spectroscopic methods. It was found that **5** converts cleanly to **6** on heating, while the isomeric **1** and **2** or **3** and **4** do not interconvert. Variable-temperature ^1H and ^{13}C NMR studies revealed that the organic ligand in **3** and **4** exists in solution as two and four isomers, respectively. Mechanistic schemes are proposed that rationalize the formation of **1** and **2** versus **3** and **4** and tentatively explain why the bulkier amine does not undergo any C–N bond cleavage. Compound **3** crystallizes in the $P\bar{1}$ space group with a = 10.967 (3) Å, b = 14.052 (4) Å, c = 8.148 (2) Å, α = 102.95 (2)°; β = 110.74 (2)°, and γ = 97.32 (3)°. Least-squares refinement based on 3358 observed reflections gave a final R value of 0.043 (R_w = 0.054). Compound **4** crystallizes in the monoclinic space group $P2_1/c$ with a = 12.223 (3) Å, b = 8.347 (1) Å, c = 21.787 (5) Å, and β = 92.93 (2)°. Least-squares refinement of 4585 observed reflections gave a final agreement factor of R = 0.041 (R_w = 0.045). Compound **5** crystallizes in the orthorhombic space group $P2_12_12_1$ with a = 15.444 (2) Å, b = 16.693 (2) Å, and c = 9.027 (1) Å. Least-squares refinement of 3706 observed reflections gave a final agreement factor of R = 0.037 (R_w = 0.039). Compound **6** crystallizes in the orthorhombic space group *Pnma* with a = 19.466 (4) Å, b = 14.610 (2) Å, and c = 8.167 (1) Å. Least-squares refinement of 3224 observed reflections gave a final agreement factor of R = 0.035 (R_w = 0.042).

Introduction

We recently reported the low-temperature (+70 °C) activation of carbon–hydrogen and carbon–nitrogen bonds in tertiary amines by $Ru_3(CO)_{12}$ promoted by $Fe_2(CO)_4(P(C_6H_5)_3)_2(\mu\text{-}SCH_2CH_3)_2$.[1] The major product from this reaction was $(\mu\text{-}H)(\mu_3\text{-}\eta^2\text{-}CH_3C{=}NCH_2CH_3)Ru_3(CO)_9$ (**1**) (eq 1). In this initial report we also noted the formation

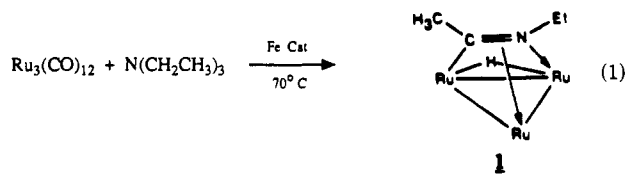

(1)

1

of three other trinuclear products but were unable to characterize these complexes due to difficulties in purification. We have now been able to obtain samples of each of these three products by successive repurifications of the reaction mixture and report here their characterization by spectroscopic techniques along with a solid-state structural investigation of two of them. Two of these products arise from coupling of a C_2 fragment to a triethylamine unit, a process that has been noted in the higher temperature catalytic transalkylation of tertiary amines by homogeneous catalysts.[2a] Because of the general relevance of these observations to the industrially important hydrodenitrification[2b] process and in order to gain some insight into the factors controlling low-temperature C–N and C–H activation processes, we thought it would be useful to extend our initial studies with triethylamine to other amines. Since C–H activation precedes C–C activation in most reactions with transition-metal clusters, we thought it would be useful to try a mixed amine containing different types of carbon–hydrogen bonds to see if we could observe some selectivity toward C–H activation that could control the course of the subsequent C–N activation processes. On the other hand, the steric bulk of the alkyl groups could be a controlling factor in the C–H and C–N activation processes. Considering these possibilities, ethyldiisopropylamine seemed a good candidate for extension of our initial studies, and we report here the results of the reaction of this amine with $Ru_3(CO)_{12}$ in the presence of catalytic amounts of $Fe_2(CO)_4(P(C_6H_5)_3)_2(\mu\text{-}SCH_2CH_3)_2$, including a solid-state structural investigation of the tri-

(1) Aime, S.; Gobetto, R.; Padovan, F.; Botta, M.; Rosenberg, E.; Gellert, R. W. *Organometallics* **1987**, *6*, 2074. For a summary of the reaction of tertiary amines with $Os_3(CO)_{12}$ see: Burgess, K. *Polyhedron* **1984**, *3*, 1175.

(2) (a) Laine, R. M. *Ann. N.Y. Acad. Sci.* **1985**, 271. (b) Satterfield, C. N.; Gultekin, S. *Ind. Eng. Chem. Proc. Des. Dev.* **1981**, *20*, 62.

0276-7333/90/2309-0913$02.50/0

Table I. Crystal Data: Collection and Refinement Parameters

	3	4	5	6
formula	$C_{17}H_{15}O_9NRu_3$	$C_{17}H_{15}O_9NRu_3$	$C_{17}H_{17}O_9NRu_3$	$C_{17}H_{15}O_9NRu_3$
formula wt	680.5	680.5	682.5	680.5
cryst syst	triclinic	monoclinic	orthorhombic	orthorhombic
space group	$P\bar{1}$	$P2_1/c$	$P2_12_12_1$	$Pnma$
a, Å	10.967 (3)	12.223 (3)	15.444 (2)	19.466 (4)
b, Å	14.052 (4)	8.347 (1)	16.963 (2)	14.610 (2)
c, Å	8.148 (2)	21.787 (5)	9.027 (1)	8.167 (1)
α, deg	101.88 (2)			
β, deg	110.74 (2)	92.93 (2)		
γ, deg	97.32 (3)			
V, Å^3	1120.4 (6)	2220 (1)	2327 (1)	2323 (1)
Z	2	4	4	4
density$_{calc}$, g/cm^3	2.017	2.036	1.945	1.946
abs coeff, μ, (cm)$^{-1}$	20.03	20.23	19.30	19.33
data collect temp, °C	21 (±1)	25 (±1)	25 (±1)	25 (±1)
radiation	Mo Kα (0.71069)	Mo Kα	Mo Kα	Mo Kα
scan mode	ω–2θ	ω	ω	ω
scan limits, deg	$2.5 < 2\theta < 50$	$4 < 2\theta < 58$	$2 < 2\theta < 67$	$2 < 2\theta < 68$
scan speed, deg/min	1.5–29.3	2–8.3	2–8.3	2–8.3
no. of data collected	4150	6415	5071	5288
no. obsd	3358	4585	3706	3224
no. of variables	271	263	271	260
R^a (R all)	0.043 (0.053)	0.041	0.037	0.035
R_w^b (R_w all)	0.053 (0.056)	0.045	0.039	0.042
largest shift/esd	0.12	0.08	0.01	0.00
weighting scheme	$1/\sigma^2$	unit weights	unit weights	$1/\sigma^2$
highest peak in final diff map, e Å^{-3}	1.6	0.70 (12)	0.42 (11)	0.51 (12)
rel trans factors	0.715–0.993	0.963–0.998	0.944–0.999	0.959–0.999

$^a R = \sum(|F_o| - |F_c|)/\sum|F_o|$. $^b R_w = [\sum w(|F_o| - |F_c|)^2/\sum w|F_o|^2]^{1/2}$.

nuclear complexes of the amine obtained.

Results and Discussion

Characterization of the Trinuclear Products from the Reaction of $Ru_3(CO)_{12}$ with Triethylamine. In addition to **1** the reaction of triethylamine with $Ru_3(CO)_{12}$ in the presence of catalytic amounts of $Fe_2(CO)_4(P(C_6H_5)_3)_2(\mu\text{-}SCH_2CH_3)_2$ gives three product bands, one that moves slightly faster than **1** on the TLC plate and two others that move slower. Subsequent repurification by TLC was necessary to obtain samples of these compounds suitable for spectroscopic analysis.

The fastest moving band, which was isolated in <5% yield, gave a parent molecular ion in the mass spectrum at 626 amu, identical with that of **1**, suggesting that this compound is an isomer of **1**. The room-temperature 270-MHz ^{1}H NMR spectrum clearly indicates the relationship between this trinuclear species and **1**. The complex exhibits a doublet of doublets at 3.55 ppm (J = 6.0 Hz, rel int = 1), a complex multiplet centered at 1.57 ppm (rel int = 2), a quartet centered at 1.32 ppm (J = 7.3 Hz, rel int = 2), a triplet at 0.95 ppm (J = 7.3 Hz, rel int = 3), and a singlet at −18.15 ppm (rel int = 1). Irradition of the doublet of doublets at 3.55 ppm causes the complex multiplet at 1.57 ppm to collapse to a simple AB pattern indicative of a methylene group with nonequivalent hydrogens. Taken together with the fact that this complex gives a ^{13}C NMR spectrum at room temperature (CO region) identical with that of **1** (197.3, 193.9, and 192.3 ppm; rel int = 1:6:2),[1] these data lead us to suggest the formula

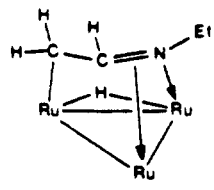

2

(μ-H)(μ_3-η^3-$CH_2CH{=}NCH_2CH_3$)$Ru_3(CO)_9$ (**2**) with the proposed structure shown. Compound **2** differs from **1** only in that oxidative addition of one C–H bond is on a carbon atom β to nitrogen instead of α to nitrogen. This structural difference has not altered the solution dynamics of **2** relative to **1** where the nitrogen oscillates between two ruthenium atoms pivoting around the σ-bound carbon atom on the third ruthenium and in concert with the edge hopping of the hydride. It is this process that causes the methylene group on nitrogen to appear as a simple quartet at ambient temperature in **1** and **2**. It is interesting to note that in spite of the similarities, the methylene group in **2** has a remarkably different chemical shift than that of **1** (1.3 versus 3.5 ppm), indicating a significant distortion of the organic ligand in order to accommodate the additional carbon atom on the cluster face.

The yellow band moving just behind **1** was recrystallized from hexane −20 °C after repurification, and a crystal suitable for crystallographic analysis was obtained. Table I lists the crystallographic data collection and refinement parameters for this complex (**3**), and Table II lists selected bond distances and bond angles. Complex **3** proved to be (μ_3-η^3-$CH_3CC(H){=}N(CH_2CH_3)_2$)$Ru_3(CO)_9$, the structure of which is illustrated in Figure 1. Compound **3** consists of a trinuclear metal core with two almost equivalent standard Ru–Ru bonds (Ru(1)–Ru(2) = 2.745 (1) Å and Ru(2)–Ru(3) = 2.786 (1) Å) and one elongated Ru–Ru bond (Ru(1)–Ru(3) = 2.952 (1) Å). From these bond lengths and the ^{1}H NMR data discussed below, we can deduce that a bridging hydride is located along the Ru(1)–Ru(3) edge of the (μ-H)$Ru_3(CO)_9$ core. The organic ligand must donate 5e$^-$ to the cluster in order to make **3** a saturated 48e$^-$ cluster. This is accomplished by 1e$^-$ σ-bond from C(2) to Ru(1) (2.075 (8) Å), a 2e$^-$ π-bond from C(2)–C(3) to Ru(2) (Ru(2)–C(2) = 2.227 (8) Å and Ru(2)–C(3) = 2.280 (7) Å), and a two-electron carbenoid bond from the zwitterionic C(4) to Ru(3) (2.092 (7) Å). The zwitterionic nature of C(4) is confirmed by the C(4)–N(5) distance of 1.303 (10) Å, indicating a carbon–nitrogen

Scheme I

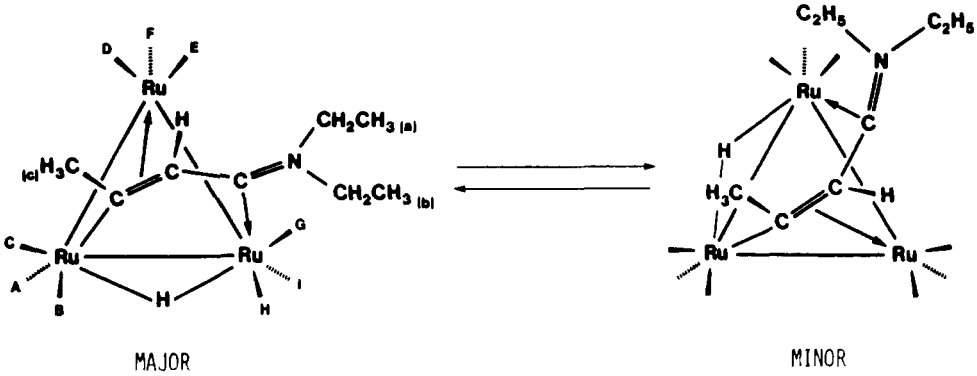

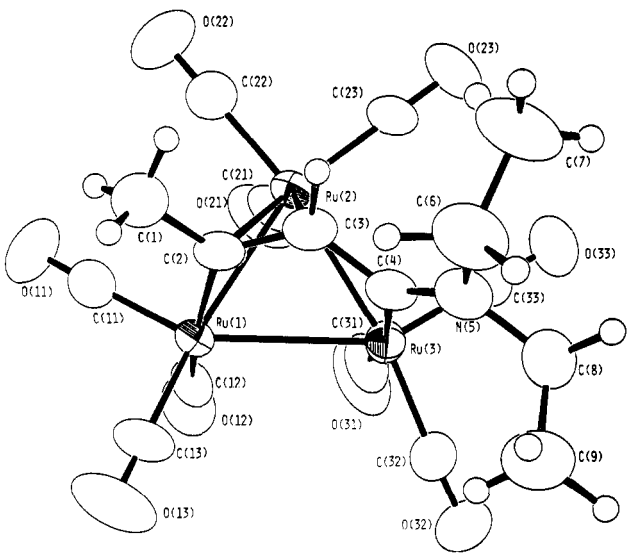

Figure 1. Solid-state structure of **3**. Hydrogen atom positions are calculated and shown to illustrate the cisoid relationship of C(1) to hydrogen on C(3).

double bond. An exactly analogous structure is formed when $CH_3C{\equiv}CCH_2N(CH_3)_2$ is reacted with $Ru_3(CO)_{12}$.[3-5] The resonance form, structure A, a 1,3-di-σ-π-allyl bonding

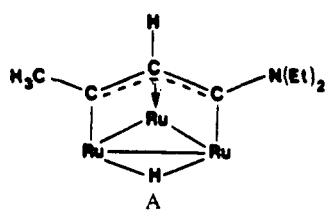

A

mode, makes only a small contribution to the ground-state structure of **3** as evidenced by the C(2)–C(3) bond length of 1.472 (10) Å along with the quoted C(4)–N(5) bond length.

The room-temperature ^1H and ^{13}C NMR spectra of **3** are entirely consistent with the solid-state structure with the additional feature that a second isomer (**3'**) is seen in a relative intensity of approximately 0.11–1.0 with **3** (see Scheme I and Table III). The NMR data for these two isomers differ only in the chemical shifts of the C–H of

(3) Aime, S.; Osella, D.; Arce, A. J.; Deeming, A. J.; Hursthouse, M. B.; Galas, A. M. R. *J. Chem. Soc., Dalton Trans.* **1984**, 1981.
(4) Aime, S.; Jannon, G.; Osella, D.; Arce, A. J.; Deeming, A. J. *J. Chem. Soc., Dalton Trans.* **1984**, 1987.
(5) Aime, S.; Osella, D.; Deeming, A. J.; Hursthouse, M. B.; Dawes, H. M. *J. Chem. Soc., Dalton Trans.* **1986**, 1459.

Table II. Bond Distances and Angles for $(\mu\text{-H})Ru_3(CO)_9(\mu_3\text{-}\eta^3\text{-}CH_3CCHC{=}N(CH_2CH_3)_2)$

Distances, Å

Ru(1)–Ru(2)	2.745 (1)	C(12)–O(12)	1.127 (11)
Ru(1)–Ru(3)	2.952 (1)	C(13)–O(13)	1.118 (9)
Ru(1)–C(11)	1.876 (11)	C(21)–O(21)	1.132 (13)
Ru(1)–C(13)	1.910 (7)	C(22)–O(22)	1.137 (13)
Ru(1)–C(12)	1.943 (9)	C(23)–O(23)	1.146 (10)
Ru(1)–C(2)	2.075 (8)	C(31)–O(31)	1.115 (13)
Ru(2)–C(21)	1.890 (10)	C(32)–O(32)	1.142 (11)
Ru(2)–C(22)	1.894 (9)	C(33)–O(33)	1.148 (10)
Ru(2)–C(23)	1.902 (7)	C(1)–C(2)	1.534 (10)
Ru(2)–C(2)	2.227 (7)	C(2)–C(3)	1.407 (11)
Ru(2)–C(3)	2.280 (7)	C(3)–C(4)	1.472 (10)
Ru(2)–Ru(3)	2.786 (1)	C(4)–N(5)	1.303 (10)
Ru(3)–C(33)	1.889 (8)	N(5)–C(6)	1.467 (11)
Ru(3)–C(32)	1.906 (9)	N(5)–C(8)	1.499 (11)
Ru(3)–C(31)	1.953 (10)	C(6)–C(7)	1.506 (12)
Ru(3)–C(4)	2.092 (7)	C(8)–C(9)	1.513 (12)
C(11)–O(11)	1.142 (15)		

Angles, deg

C(11)–Ru(1)–C(13)	97.8 (4)	N(5)–C(6)–C(7)	111.3 (8)
C(11)–Ru(1)–C(12)	87.7 (4)	N(5)–C(8)–C(9)	110.1 (7)
C(11)–Ru(1)–C(2)	92.0 (4)	C(33)–Ru(3)–C(32)	98.7 (4)
C(11)–Ru(1)–Ru(2)	94.4 (3)	C(33)–Ru(3)–C(31)	92.4 (4)
C(11)–Ru(1)–Ru(3)	150.4 (3)	C(33)–Ru(3)–C(4)	88.0 (3)
C(13)–Ru(1)–C(12)	97.0 (4)	C(33)–Ru(3)–Ru(2)	91.6 (2)
C(13)–Ru(1)–C(2)	100.7 (3)	C(33)–Ru(3)–Ru(1)	148.4 (2)
C(13)–Ru(1)–Ru(2)	151.3 (3)	C(32)–Ru(3)–C(31)	90.8 (4)
C(13)–Ru(1)–Ru(3)	111.8 (3)	C(32)–Ru(3)–C(4)	101.3 (3)
C(12)–Ru(1)–C(2)	162.2 (3)	C(32)–Ru(3)–Ru(2)	166.4 (3)
C(12)–Ru(1)–Ru(2)	109.4 (2)	C(32)–Ru(3)–Ru(1)	112.9 (3)
C(12)–Ru(1)–Ru(3)	90.5 (2)	C(31)–Ru(3)–C(4)	167.8 (3)
C(2)–Ru(1)–Ru(2)	52.8 (2)	C(31)–Ru(3)–Ru(2)	97.7 (3)
C(2)–Ru(1)–Ru(3)	80.9 (2)	C(31)–Ru(3)–Ru(1)	88.0 (3)
Ru(2)–Ru(1)–Ru(3)	58.41 (2)	C(4)–Ru(3)–Ru(2)	70.1 (2)
C(21)–Ru(2)–C(22)	93.5 (4)	C(4)–Ru(3)–Ru(1)	85.3 (2)
C(21)–Ru(2)–C(23)	99.2 (4)	Ru(2)–Ru(3)–Ru(1)	57.08 (2)
C(21)–Ru(2)–C(2)	129.5 (3)	O(11)–C(11)–Ru(1)	178.2 (10)
C(21)–Ru(2)–C(3)	156.3 (3)	O(12)–C(12)–Ru(1)	177.6 (8)
C(21)–Ru(2)–Ru(1)	83.6 (2)	O(13)–C(13)–Ru(1)	178.1 (10)
C(21)–Ru(2)–Ru(3)	89.2 (3)	O(21)–C(21)–Ru(2)	177.9 (8)
C(22)–Ru(2)–C(23)	95.0 (4)	O(22)–C(22)–Ru(2)	175.7 (10)
C(22)–Ru(2)–C(2)	88.2 (3)	O(23)–C(23)–Ru(2)	179.5 (7)
C(22)–Ru(2)–C(3)	103.1 (4)	O(31)–C(31)–Ru(3)	175.4 (8)
C(22)–Ru(2)–Ru(1)	105.9 (3)	O(32)–C(32)–Ru(3)	176.6 (9)
C(22)–Ru(2)–Ru(3)	169.7 (3)	O(33)–C(33)–Ru(3)	178.5 (8)
C(23)–Ru(2)–C(2)	130.9 (3)	C(3)–C(2)–C(1)	112.5 (7)
C(23)–Ru(2)–C(3)	96.1 (3)	C(3)–C(2)–Ru(1)	124.9 (5)
C(23)–Ru(2)–Ru(1)	158.7 (2)	C(3)–C(2)–Ru(2)	73.9 (4)
C(23)–Ru(2)–Ru(3)	94.3 (2)	C(1)–C(2)–Ru(1)	122.5 (6)
C(2)–Ru(2)–C(3)	36.4 (3)	C(1)–C(2)–Ru(2)	122.6 (5)
C(2)–Ru(2)–Ru(1)	47.9 (2)	Ru(1)–C(2)–Ru(2)	79.2 (3)
C(2)–Ru(2)–Ru(3)	82.4 (2)	C(2)–C(3)–C(4)	123.3 (6)
C(3)–Ru(2)–Ru(1)	75.6 (2)	C(2)–C(3)–Ru(2)	69.8 (4)
C(3)–Ru(2)–Ru(3)	71.6 (2)	C(4)–C(3)–Ru(2)	96.9 (4)
Ru(1)–Ru(2)–Ru(3)	64.51 (2)	N(5)–C(4)–C(3)	117.5 (6)
C(4)–N(5)–C(6)	122.5 (7)	N(5)–C(4)–Ru(3)	129.0 (5)
C(4)–N(5)–C(8)	124.4 (7)	C(3)–C(4)–Ru(3)	113.1 (5)
C(6)–N(5)–C(8)	113.0 (7)		

Table III. ^1H and ^{13}C NMR Data for 3 and 3′ in $CDCl_3$[a,b]

	^1H NMR, ppm							^{13}C NMR,[c] ppm		
compd	hydride	C-H	CH_3(c)	CH_3(a)	CH_3(b)	CH_2(a)	CH_2(b)	Ru(1)	Ru(2)	Ru(3)
3	−17.7 (d (1), J = 2.6 Hz)	6.02 (d (1), J = 2.6 Hz)	2.79 (s (3))	1.31 (t, (3), J = 7.15 Hz)	1.38 (t (3), J = 7.15 Hz)	3.56 (m)	3.74 (m)	199.8 (A)	192.1 (D)	191.9 (G)
						3.85 (m, (2), J = 4.7 Hz)	4.22 (m, (2), J = 4.7 Hz)	189.5 (B)	193.9 (E)	195.7 (H)
								194.5 (C)	197.9 (F)	207.9 (E)
3′	−17.92 (d (1), J = 3.0 Hz)	5.96 (d (1), J = 3.0 Hz)	2.79 (s (3))	1.31 (t, (3), J = 7.15 Hz)	1.38 (t (3), J = 7.15 Hz)	3.56 (m)	3.74 (m)			
						3.85 (m (2), J = 4.7 Hz)	4.22 (m (2), J = 4.7 Hz)			

[a] Letters in parentheses refer to Scheme I. [b] Relative intensity for each isomer in parentheses. [c] Data given for low-temperature limit (−65 °C), assignments for equatorials on Ru(2) and Ru(3) are interchangeable, all rel int = 1. Resonance B $J(^1H-^{13}CO)$ = 4.23 Hz, C $J(^1H-^{13}CO)$ = 12.1 Hz.

Table IV. Bond Distances and Angles for $(\mu\text{-H})(\mu_3\text{-}\eta^3\text{-}(CH_3CH_2)_2N{=}C(H)C(H)CCH_2)Ru_3(CO)_9$ (4)[a]

Distances, Å

Ru1-Ru2	2.853 (1)	O13-C13	1.13 (1)	Ru2-C21	1.91 (1)	C1-C2	1.41 (1)
Ru1-Ru3	2.877 (1)	O21-C21	1.13 (1)	Ru2-C22	1.88 (1)	C1-H1	0.95
Ru1-C1	2.27 (1)	O22-C22	1.15 (1)	Ru2-C23	1.90 (1)	C1-H2	0.95
Ru1-C2	2.38 (1)	O23-C23	1.13 (1)	Ru3-C2	2.11 (1)	C2-C3	1.46 (1)
Ru(1)-C11	1.90 (1)	O31-C31	1.12 (1)	Ru3-C31	1.92 (1)	C3-C4	1.39 (1)
Ru1-C12	1.90 (1)	O32-C32	1.13 (1)	Ru3-C32	1.95 (1)	C3-H3	0.95
Ru1-C13	1.91 (1)	O33-C33	1.14 (1)	Ru3-C33	1.88 (1)	C4-H4	0.95
Ru1-H	1.85	N-C4	1.32 (1)	O11-C11	1.14 (1)	C7-C8	1.50 (1)
Ru2-Ru3	2.746 (1)	N-C5	1.52 (1)	O12-C12	1.12 (1)		
Ru2-C3	2.28 (1)	N-C7	1.46 (1)				

Angles, deg

Ru2-Ru1-Ru3	57.27 (2)	C12-Ru1-C13	93.9 (3)	Ru1-Ru3-C33	147.0 (3)	H1-C1-H2	120.0 (7)
Ru2-Ru1-C1	90.6 (2)	C12-Ru1-H	85.4 (2)	Ru1-Ru3-H	38.99 (1)	Ru1-C2-Ru2	70.6 (2)
Ru2-Ru1-C2	57.4 (2)	C13-Ru1-H	85.0 (2)	Ru2-Ru3-C2	61.7 (2)	Ru1-C2-Ru3	79.5 (2)
Ru2-Ru1-C11	88.0 (2)	Ru1-Ru2-Ru3	61.79 (2)	Ru2-Ru3-C31	161.3 (3)	Ru1-C2-C1	67.9 (4)
Ru2-Ru1-C12	90.7 (2)	Ru1-Ru2-C3	77.4 (2)	Ru2-Ru3-C32	100.4 (2)	Ru1-C2-C3	112.9 (4)
Ru2-Ru1-C13	174.0 (2)	Ru1-Ru2-C21	100.5 (2)	Ru2-Ru3-C33	89.6 (2)	Ru3-C2-C1	119.2 (5)
Ru2-Ru1-H	91.46 (2)	Ru1-Ru2-C22	88.3 (2)	Ru2-Ru3-H	94.85 (2)	Ru3-C2-C3	122.9 (4)
Ru3-Ru1-C1	71.7 (2)	Ru1-Ru2-C23	160.6 (2)	C2-Ru3-C31	99.6 (3)	C1-C2-C3	116.8 (6)
Ru3-Ru1-C2	46.1 (1)	Ru3-Ru2-C3	76.9 (1)	C2-Ru3-C32	157.3 (3)	Ru2-C3-C2	82.7 (4)
Ru3-Ru1-C11	141.4 (2)	Ru3-Ru2-C21	160.9 (2)	C2-Ru3-C33	100.0 (3)	Ru2-C3-C4	94.7 (4)
Ru3-Ru1-C12	103.2 (2)	Ru3-Ru2-C22	90.5 (2)	C2-Ru3-H	86.1 (2)	Ru2-C3-H3	93.2 (4)
Ru3-Ru1-C13	117.7 (2)	Ru3-Ru2-C23	98.9 (2)	C31-Ru3-C32	97.3 (4)	C2-C3-C4	122.5 (5)
Ru3-Ru1-H	39.04 (2)	C3-Ru2-C21	92.8 (3)	C31-Ru3-C33	95.3 (4)	C2-C3-H3	118.7 (6)
C1-Ru1-C2	35.2 (2)	C3-Ru2-C22	164.2 (3)	C31-Ru3-H	81.9 (3)	C4-C3-H3	118.8 (6)
C1-Ru1-C11	94.4 (3)	C3-Ru2-C23	100.9 (3)	C32-Ru3-C33	93.3 (4)	N-C4-C3	126.5 (6)
C1-Ru1-C12	172.9 (3)	C21-Ru2-C22	96.5 (3)	C32-Ru3-H	81.4 (2)	N-C4-H4	117.2 (6)
C1-Ru1-C13	84.4 (3)	C21-Ru2-C23	98.9 (3)	C33-Ru3-H	173.6 (3)	C3-C4-H4	116.3 (6)
C1-Ru1-H	87.7 (2)	C22-Ru2-C23	90.3 (3)	C4-N-C5	123.4 (6)	N-C5-C6	113.2 (6)
C2-Ru1-C11	102.9 (3)	Ru1-Ru3-Ru2	60.93 (2)	C4-N-C7	122.2 (6)	N-C7-C8	111.8 (7)
C2-Ru1-C12	143.3 (3)			C5-N-C7	114.2 (6)		
C2-Ru1-C13	117.0 (3)			Ru1-C1-C2	77.0 (4)		
C2-Ru1-H	78.5 (1)			Ru1-C1-H1	99.3 (5)		
C11-Ru1-C12	92.6 (3)			Ru1-C11-O11	176.9 (7)	Ru2-C23-O23	176.9 (7)
C11-Ru1-C13	95.7 (3)			Ru1-C12-O12	173.9 (7)	Ru3-C31-O31	176.6 (8)
C11-Ru1-H	177.9 (2)			Ru1-C13-O13	176.5 (7)	Ru3-C32-O32	178.1 (7)
Ru1-Ru3-C2	54.5 (2)	Ru1-C1-H2	93.8 (5)	Ru2-C21-O21	177.5 (7)	Ru3-C33-O33	176.2 (7)
Ru1-Ru3-C31	108.4 (3)	C2-C1-H1	119.7 (6)	Ru2-C22-O22	175.3 (7)	Ru1-H-Ru3	101.96 (2)
Ru1-Ru3-C32	105.6 (2)	C2-C1-H2	120.3 (6)				

[a] Numbers in parentheses are estimated standard deviations in the least significant digits.

the hydrocarbon ligand and hydride signals. We suggest that these isomers differ only in the relative orientation of the CH_3 and the hydrogen on C(3) around the C(2)–C(3) double bond, transoid in 3′ (minor isomer) and cisoid in 3 (major isomer, Scheme I). These isomers do not interchange on the NMR time scale up to +60 °C in $CDCl_3$.

The variable-temperature ^{13}C NMR spectrum of 3 shows only localized axial–radial exchanges at Ru(2) and Ru(3) from the low-temperature limit to +40 °C with the carbonyls on Ru(1) remaining rigid throughout this temperature range. The assignments (Scheme I and Table III) given are based on the observed hydride couplings and by analogy with the dimethylamino analogue, which shows the same temperature dependence.[5] The resonance of the carbonyl trans to the zwitterionic carbon shows an exceptionally low field chemical shift for a terminal ruthenium-bound CO, consistent with strong donor ability of the carbenoid ligand.[6]

The third product isolated in 10% yield after repurification based on consumed ruthenium carbonyl also appears to be the result of coupling of a C_2 fragment with a triethylamine group on the basis of its mass spectrum alone, which shows a parent molecular ion at 681 amu consistent with this having the molecular formula $HRu_3(CO)_9((CH_3CH_2)_2N{=}C_4H_4)$ (4) and being an isomer of 3.

(6) For examples of other carbenoid cluster complexes see: Adams, R. D.; Balin, J. E. *Organometallics* **1988**, *7*, 963.

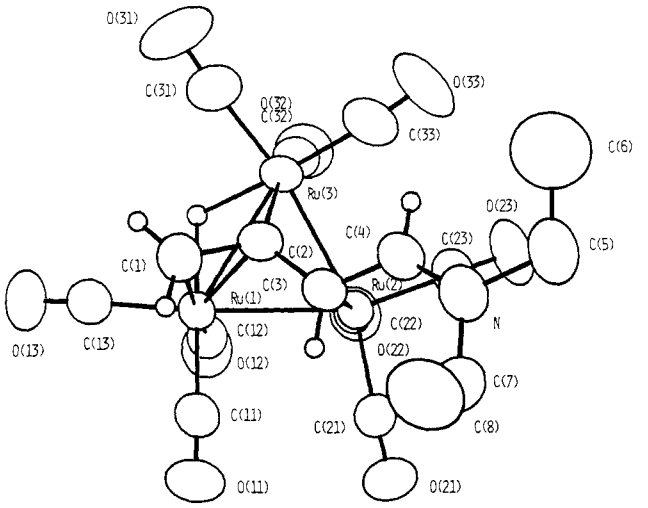

Figure 2. Solid-state structure of **4**. Hydrogen atom positions are calculated and shown to illustrate their relative orientation in the organic ligand.

A crystal suitable for crystallographic analysis was obtained from hexane by slow evaporation at room temperature. Table I lists the crystallographic data collection and refinement parameters, and Table IV lists selected bond distances and angles. Compound **4** proved to be $(\mu\text{-H})(\mu_3\text{-}\eta^3\text{-}(CH_3CH_2)_2N{=}C(H)C(H)CCH_2)Ru_3(CO)_9$, the structure of which is shown in Figure 2. Compound **4** consists of a trinuclear metal core with two almost equivalent elongated Ru–Ru bonds (Ru(1)–Ru(2) = 2.853 (1) Å and Ru(1)–Ru(3) = 2.877 (1) Å) and one slightly shortened Ru–Ru bond (Ru(2)–Ru(3) = 2.746 (1) Å). From these bond lengths and the ^{1}H NMR data discussed below, we deduce that the bridging hydride is located along the Ru(1)–Ru(3) edge of the $(\mu\text{-H})Ru_3(CO)_9$ core. The organic ligand must donate 5e$^-$ to the cluster in order to make **4** a saturated cluster. This is accomplished by a 3e$^-$ σ-π-vinyl bonding of C(1)–C(2) disposed over the Ru(1)–Ru(3) edge (σ to Ru(3) and π to Ru(1)) and a 2e$^-$ carbenoid bond from C(3) to Ru(2). This bonding scheme is directly analogous to that found for the related complexes $HM_3(CO)_9(\mu_3\text{-}\eta^3\text{-}(CH_3)_2NCC{=}CH_2)$ (M = Ru, Os) obtained from the reactions of aminoalkynes with the parent carbonyls.[5] The location of C(3) directly over Ru(2) and the C(4)–Ru(2) distance of 2.77 Å clearly suggest that the C(4)=N(Et)$_2$ group is not bound to the cluster. The C(1)–C(2) bond length of 1.41 (1) Å is typical for σ-π-vinyl complexes,[5] while the C(2)–C(3) and C(3)–C(4) bond lengths of 1.46 (1) and 1.39 (1) Å are suggestive of π-electron delocalization throughout the ligand, with the C(3)–C(4) bond having somewhat more double-bond character than the C(2)–C(3) bond. The C(4)–N bond length of 1.32 (1) Å indicates a carbon–nitrogen double bond.

The variable-temperature ^{1}H NMR of this complex is shown in Figure 3. At the low-temperature limit (−40 °C) we observe two major isomers in approximately equal population as evidenced by the presence of (1) two olefinic hydrogen doublets at 7.4 and 7.1 ppm (J = 10.7 Hz, rel int = 1 each), which are coupled with two doublet resonances at 3.2 and 2.6 ppm, respectivley (rel int = 1 each); (2) two singlets at 2.64 and 2.73 ppm (rel int = 1 each); (3) a doublet at 2.06 ppm (J = 1.8 Hz, rel int = 1) with a companion singlet at 1.85 ppm (rel int = 1); (4) two rel int = 1 resonances in the hydride region at −16.0 and at −17.7 ppm, the last coupled with the doublet at 2.06 ppm; (5) two sets of ethyl group methyl resonances at 1.4 ppm (rel int = 3) and 1.2 ppm (rel int = 3) with companion AB multiplets at 3.2 and 3.5 ppm (rel int = 2 each). Each of these pairs of resonances (except for the ethyl group resonances) average with each other as the temperature is increased to +60 °C. We can also detect the presence of

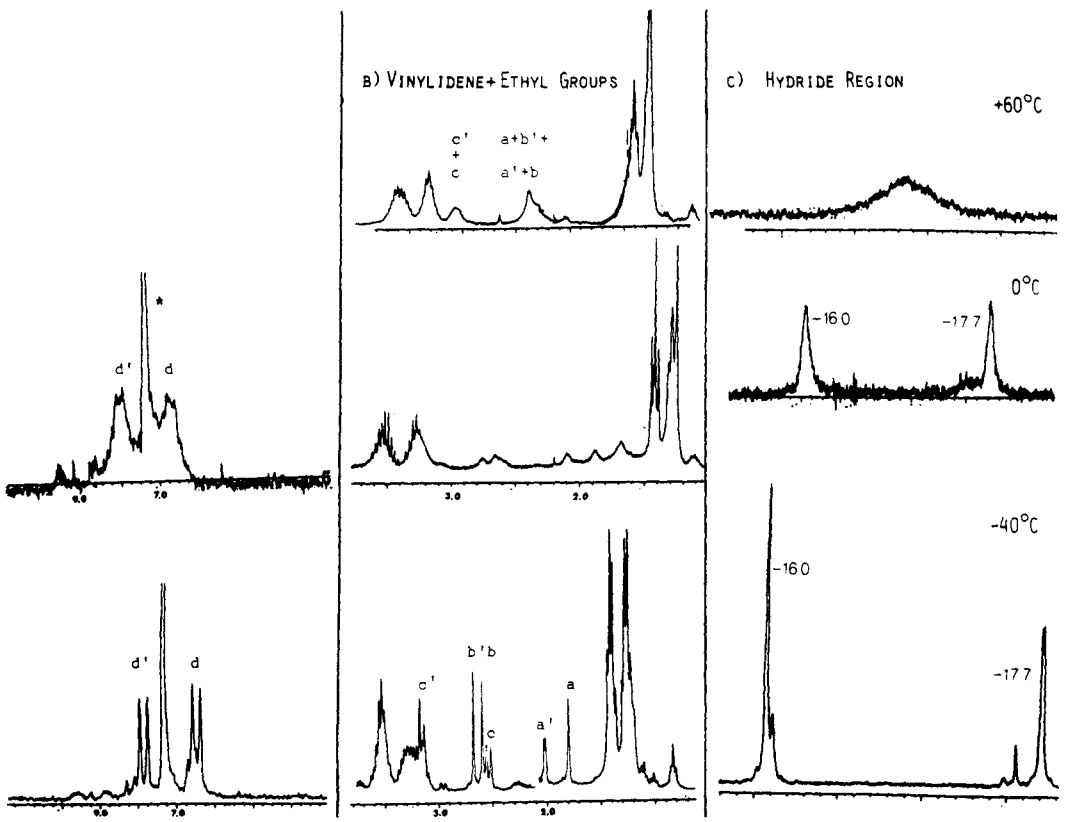

Figure 3. Variable-temperature ^{1}H NMR of **4** from −40 to +60 °C in $CDCl_3$ at 270 MHz. Letters refer to Scheme II and are interchangeable for the two major isomers. Spectra at 0 °C are at slightly different scales.

Scheme II

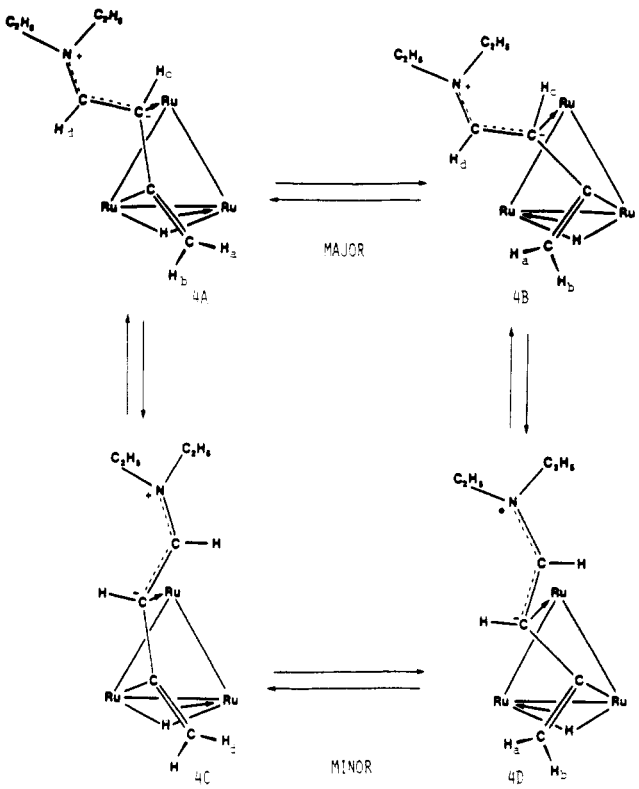

two additional isomers in the olefinic and hydride regions (Figure 3). The proposed structures for the four related isomers are shown in Scheme II, and the resonances are assigned in Figure 3 using the notation in the scheme. The two major isomers **4A** and **4B** should have the same ligand geometry as that found in the solid state (Scheme II). It should be pointed out that the chemical shifts of the vinylidenic hydrogens in the related complexes $HM_3(CO)_9(\mu_3\text{-}\eta^3\text{-}(CH_3)_2NCC{=}CH_2)$ (M = Ru, Os) are very similar to those observed for **4**.[5] In the ruthenium complex a $^4J(^1H\text{-}^1H)$ = 1.8 Hz is observed between the hydride and one of the vinylidenic hydrogens, while in the osmium analogue two singlets are observed for the vinylidenic hydrogens. We suggest that these isomers differ from each other by a 90° change in the dihedral angle made between the vinylidenic CH_2 plane and the Ru_2H plane. The similarity in chemical shift between hydrides in each major–minor isomer pair (**4A–4C** and **4B–4D**) and the similar populations of **4A** and **4B** and of **4C** and **4D** are also consistent with these assignments. The observed fluxionality of **4** is similar in barrier height to that observed for the complexes $HM_3(CO)_9(\mu_3\text{-}\eta^3\text{-}(CH_3)_2NC{=}C{=}CH_2)$[5]. The ^{13}C NMR spectrum of a ^{13}CO-enriched sample of **4** shows 17 carbonyl resonances of approximately equal intensity (one of relative intensity 2) as expected from the chiral structure of the two major isomers. Some lower intensity resonances are also observed that are assigned to the minor isomers (see experimental for ^{13}C NMR data). The overall bonding scheme for the organic ligand in **4** is similar to that observed for **3**, being a five-electron donor with one σ-, one π-metal interaction, and one zwitterionic carbenoid interaction (Scheme II).[6] This η^3 ligand is apparently much more fluxional than the η^3 ligand in **3**.

Characterization of the Trinuclear Products from the Reaction of $Ru_3(CO)_{12}$ with Ethyldiisopropylamine. The reaction of ethyldiisopropylamine with $Ru_3(CO)_{12}$ in the presence of the iron dimer catalyst gives two trinuclear amine-containing products. The complexes were purified by TLC and characterized by infrared, mass,

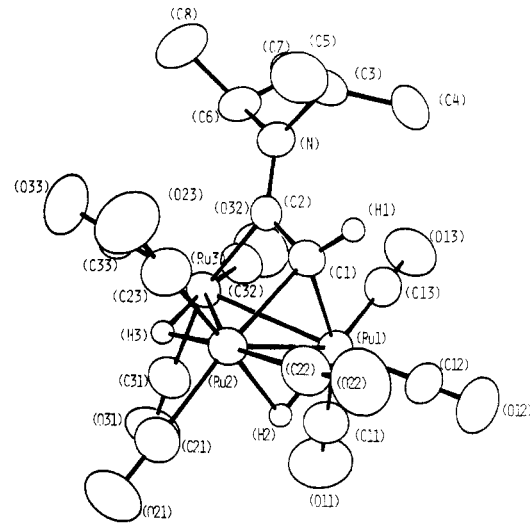

Figure 4. Solid-state structure of **5** showing the calculated positions of the two hydrides.

and ^1H and ^{13}C NMR spectroscopies. Solid-state structural investigations were completed on both complexes.

The faster moving TLC band proved to be $(\mu\text{-}H)_2(\mu_3\text{-}\eta^2\text{-}HCC{=}N(CH(CH_3)_2)_2Ru_3(CO)_9$ (**5**). The solid-state structure of **5** is shown in Figure 4, the crystal data are given in Table I, and selected bond distances and bond angles are given in Table V. The structure consists of an $H_2Ru_3(CO)_9$ core with the location of the hydrides inferred from the longer Ru(1)–Ru(2) (2.8058 (9) Å) and Ru(2)–Ru(3) (2.9529 (9) Å) bonds and from the ^1H and ^{13}C NMR data discussed below. The exact locations of the hydrides were calculated by using the Hydex potential energy minimum program.[7] The cluster requires a $4e^-$ donor to have the required $48e^-$ for a saturated Ru_3 cluster. This occurs by having two $1e^-$ σ-bonds from C(1) to Ru(1) (2.154 (2) Å) and C(1) to Ru(2) (2.148 (7) Å) and a $2e^-$ carbenoid bond from C(2) to Ru(3) (2.100 (7) Å). This description of the bonding is clearly the major contribution to the ground-state structure with the C–N bond length of 1.330 (9) Å indicating a zwitterionic C–N double bond and the location of C(2) directly over Ru(3) suggesting little direct π-donation from any C(1)–C(2) π-electron density. However, the C(1)–C(2) bond length of 1.44 (1) Å clearly indicates some double-bond character, and the orientation of the isopropyl groups indicates that π-electron density for the C(1)-C(2) bond is in a plane perpendicular to the plane of the Ru_3 triangle. As for **3** and **4** there is no evidence for a direct C=N—Ru(3) π-interaction. The variable-temperature ^1H NMR of **5** in acetone-d_6 shows two hydrides at −14.49 and −18.38 ppm in the low-temperature limiting spectrum (−35 °C), which broaden and coalesce at 0 °C ($\Delta G^\ddagger$ = 11.2 kcal/mol[8]) and then emerge as a single resonance at −16.34 ppm at 23 °C. The hydrogen atom on C(1) shows a singlet in the olefinic region at 6.23 ppm, and the two nonequivalent isopropyl groups show the expected septuplets at 4.79 and 4.22 ppm and doublets at 1.64 and 1.47 ppm (J = 6.94 and 7.33 Hz). To understand the relationship between the observed hydride exchange and any possible motions of the carbons on the organic ligand, we investigated the variable-temperature ^{13}C NMR spectrum of a ^{13}CO-enriched sample of **5**. The low-temperature limiting spectrum is reached at −92 °C and shows

(7) Orpen, A. G. *J. Chem. Soc., Dalton Trans.* **1980**, 2509.
(8) $\Delta G^\ddagger$ estimated from coalescence temperature using the equation $\Delta G_c^\ddagger = 4.57(T_c)(9.97 - \log T_c/\delta\nu)$: Kost, D.; Carlson, E. H.; Ruban, M. *J. Chem. Soc., Chem. Commun.* **1971**, 656.

Table V. Bond Distances and Angles for $(\mu\text{-H})_2(\mu_3\text{-}\eta^2\text{-HCC=N(CH(CH}_3)_2)_2\text{Ru}_3(\text{CO})_9$ (5)[a]

	Distances, Å		
Ru1-Ru2	2.8059 (9)	O11-C11	1.13 (1)
Ru1-Ru3	2.7557 (9)	O13-C13	1.14 (1)
Ru1-C1	2.146 (8)	O12-C12	1.11 (1)
Ru1-C11	1.94 (1)	O21-C21	1.13 (1)
Ru1-C13	1.07 (1)	O22-C22	1.12 (1)
Ru1-C12	1.939 (9)	O23-C23	1.14 (1)
Ru1-H2	1.85	O31-C31	1.12 (1)
Ru2-Ru3	2.9531 (8)	O32-C32	1.14 (1)
Ru2-C1	2.140 (6)	O33-C33	1.14 (1)
Ru2-C21	1.950 (8)	N-C2	1.330 (9)
Ru2-C22	1.916 (9)	N-C3	1.498 (9)
Ru2-C23	1.886 (9)	N-C6	1.48 (1)
Ru2-H2	1.85	C1-C2	1.43 (1)
Ru2-H3	1.85	C1-H1	1.06
Ru3-C2	2.103 (7)	C3-C4	1.55 (1)
Ru3-C31	1.948 (9)	C3-C5	1.52 (1)
Ru3-C32	1.880 (9)	C6-C7	1.54 (1)
Ru3-C33	1.912 (9)	C6-C8	1.54 (1)
Ru3-H3	1.85		
	Angles, deg		
Ru2-Ru1-Ru3	64.14 (2)	Ru1-Ru2-C23	141.8 (3)
Ru2-Ru1-C1	49.0 (2)	Ru1-Ru2—H2	40.73 (2)
Ru2-Ru1-C11	117.3 (3)	Ru1-Ru2-H3	92.12 (3)
Ru2-Ru1-C13	141.0 (3)	Ru3-Ru2-C1	64.3 (2)
Ru2-R1-C12	99.5 (3)	Ru3-Ru2-C21	109.1 (2)
Ru2-Ru1-H2	40.72 (2)	Ru3-Ru2-C22	148.2 (3)
Ru3-Ru1-C1	68.3 (2)	Ru3-Ru2-C23	103.1 (3)
Ru3-Ru1-C11	95.3 (3)	Ru3-Ru2-H2	78.60 (2)
Ru3-Ru1-C13	94.7 (3)	Ru3-Ru2-H3	37.09 (2)
Ru3-Ru1-C12	162.5 (3)	C1-Ru2-C21	169.6 (3)
Ru3-Ru1-H2	84.17 (3)	O1-Ru2-C22	87.4 (3)
C1-Ru1-C11	161.7 (4)	C1-Ru2-C23	93.6 (3)
C1-Ru1-C13	93.6 (3)	C1-Ru2-H2	88.9 (2)
C1-Ru1-C12	96.7 (3)	C1-Ru2-H3	95.8 (2)
C1-Ru1-H2	88.7 (2)	C21-Ru2-C22	96.6 (3)
C11-Ru1-C13	95.9 (4)	C21-Ru2-C23	95.8 (4)
C11-Ru1-C12	98.1 (4)	C21-Ru2-H2	81.7 (3)
C11-Ru1-H2	81.3 (3)	C21-Ru2-H3	81.2 (2)
C13-Ru1-C12	95.1 (4)	C22-Ru2-C23	92.2 (4)
C13-Ru1-H2	176.9 (3)	C22-Ru2-H2	87.2 (3)
C12-Ru1-H2	86.8 (3)	C22-Ru2-H3	173.8 (3)
Ru1-Ru2-Ru3	57.11 (2)	C23-Ru2-H2	177.4 (3)
Ru1-Ru2-C1	49.2 (2)	C23-Ru2-H3	82.3 (3)
Ru1-Ru2-C21	120.7 (3)	H2-Ru2-H3	98.14 (3)
Ru1-Ru2-C22	94.0 (3)	Ru1-Ru3-Ru2	58.76 (2)
Ru1-Ru3-C2	68.3 (2)	Ru1-C1-H1	117.4 (5)
Ru1-Ru3-C31	93.4 (3)	Ru2-C1-O1	198.8 (5)
Ru1-Ru3-C32	90.6 (3)	Ru2-C1-H1	125.4 (5)
Ru1-Ru3-C33	165.3 (2)	C2-C1-H1	116.2 (6)
Ru1-Ru3-H3	93.71 (13)	Ru3-C2-N	133.0 (5)
Ru2-Ru3-C2	68.5 (2)	Ru3-C2-C1	102.9 (4)
Ru2-Ru3-C31	95.5 (3)	N-C2-C1	123.9 (6)
Ru2-Ru3-C32	148.3 (3)	N-C3-C4	111.5 (7)
Ru2-Ru3-C33	112.6 (3)	N-C3-C5	112.9 (6)
Ru2-Ru3-H3	37.07 (2)	C4-C3-C5	114.5 (7)
C2-Ru3-C31	160.0 (3)	N-C6-C7	111.3 (7)
C2-Ru3-C32	94.3 (3)	N-C6-C8	110.4 (7)
C2-Ru3-C33	99.7 (3)	C7-C6-C8	113.6 (8)
C2-Ru3-H3	91.6 (2)	Ru1-C11-O11	178 (1)
C31-Ru3-C32	94.0 (3)	Ru1-C13-O13	179.2 (8)
C31-Ru3-C33	97.5 (4)	Ru1-C12-O12	180 (1)
C31-Ru3-H3	81.2 (3)	Ru2-C21-O21	178.3 (8)
C32-Ru3-C33	96.0 (4)	Ru2-C22-O22	174.3 (8)
C32-Ru3-H3	173.7 (3)	Ru2-C23-O23	178.4 (9)
C33-Ru3-H3	80.7 (3)	Ru3-C31-O31	176.6 (8)
C2-N-C3	123.8 (6)	Ru3-C32-O32	178.3 (8)
C2-N-C6	120.3 (6)	Ru3-C33-O33	176.0 (8)
C3-N-C6	115.8 (6)	Ru1-H2-Ru2	98.55 (3)
Ru1-C1-Ru2	81.8 (2)	Ru2-H3-Ru3	105.83 (3)
Ru1-C1-C2	100.1 (5)		

[a] Numbers in parentheses are estimated standard deviations in the least significant digits.

eight resonances at 198.6 (1), 196.8 (2), 196.5 (1), 194.8 (1), 189.7 (1), 187.5 (1), 185.5 (1), and 183.4 (1) ppm, consistent with the solid-state structure if one allows for accidental overlap of two resonances (Figure 5). As the temperature is increased to −68 °C all the resonances except one of the two overlapping resonances at 196.8 ppm broaden and at −47 °C the two resonances at 185.5 and 183.4 ppm have averaged to a single resonance at 184.6 ppm. At 0 °C, the temperature at which the hydrides just begin to coalesce, one hydride is already rapidly edge hopping on the NMR time scale, and five sharp resonances are observed at 196.8 (1), 194.9 (2), 191.8 (2), 191.4 (2), and 184.6 (2) ppm, consistent with C_s symmetry for the molecule at 0 °C. The five resonances arise from averaging of pairs of resonances from the low-temperature limiting spectrum (see Figure 5), and thus the barrier for this process can be estimated to be 9.2 kcal/mol.[8] At +23 °C where both hydrides are moving on the NMR time scale, we begin to observe broadening of six carbonyl groups while the remaining three are sharp. There is thus a two-stage hydride migration. From −92 to −35 °C simple edge hopping of one hydride from the Ru(2)–Ru(3) edge to the Ru(1)–Ru(3) edge pivoting on Ru(3) occurs, while above −35 °C both hydrides begin to migrate around the Ru_3 triangle. This type of two-stage hydride exchange has been previously observed in a variety of triosmium and triruthenium clusters containing two hydride ligands.[9,10] Throughout the temperature range examined (−92 to +23 °C) there is no evidence of rotation of the organic ligand, in contrast with other face-capped dihydrides that have been exam-

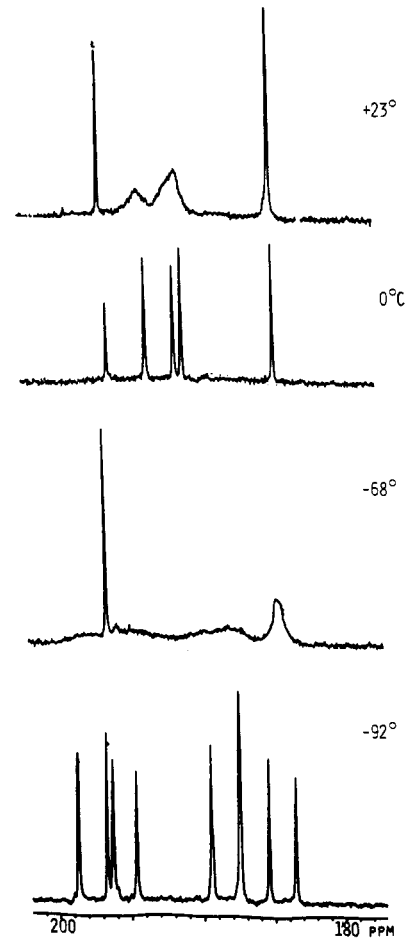

Figure 5. Variable-temperature ^{13}C NMR of the carbonyl region of **5** in CD_2Cl_2 from −92 to 23 °C at 68 MHz.

(9) Keister, J. B.; Churchill, M. R.; Jank, T. S.; Duggan, T. P. *Organometallics* **1987**, *6*, 799.
(10) Deeming, A. J. *Adv. Organomet. Chem.* **1986**, *26*, 1.

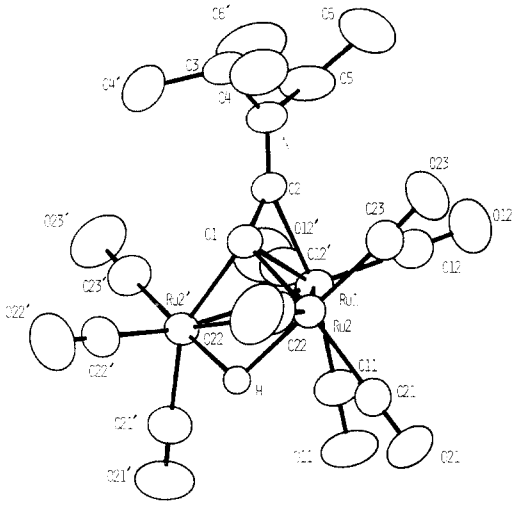

Figure 6. Solid-state structure of **6** showing the calculated position of the hydride ligand.

ined where the organic ligand migrates over the face of the cluster.[9,10] An osmium analogue of **5** has recently been synthesized by Adams et al.[11] by a three-step synthesis starting from $Os_3(CO)_{10}(CH_3CN)_2$ and triethylamine, building on the earlier work of Shapley[12] (eq 2).

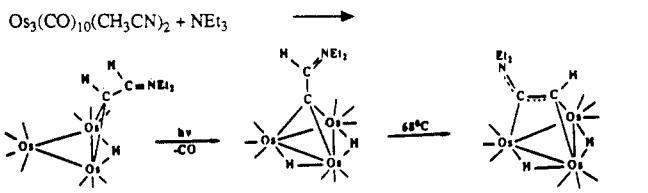

(2)

The solid-state structure of the second amine-containing triruthenium product $(\mu\text{-H})(\mu_3\text{-}\eta^2\text{-CC=N(CH(CH}_3)_2)_2)\text{Ru}_3(\text{CO})_9$ (**6**) is shown in Figure 6. Crystal data are given in Table I, and selected bond distances and bond angles are listed in Table VI. The molecule consists of a $(\mu\text{-H})\text{Ru}_3(\text{CO})_9$ core with two different Ru–Ru distances (Ru(2)-Ru(2′) = 2.8578 (4) Å, and Ru(1)–Ru(2) and Ru(1)–Ru(2′) = 2.7807 (4) Å). The hydridic hydrogen atom was located on the longest Ru–Ru edge; its position was defined by the program HYDEX[7] and by consideration of the Ru–CO skeletal geometry (Figure 6). Five electrons are required from the organic ligand, and its bonding to the triruthenium core can be described as a $1e^-$ σ-bond and a $2e^-$ carbenoid bond, both from the zwitterionic C(1) interchangeably to Ru(2) or Ru(2′). Since the C(1)–Ru(2) and C(1)–Ru(2′) bond lengths are the same (2.030 (3) Å) because the molecule sits on a mirror plane, it is best to view this interaction as a three center–three electron bond. The other two electrons required from the ligand come from a $2e^-$ π-interaction from the apparent C(1)–C(2) double bond (C(1)–C(2) = 1.341 (6) Å). The C(2)–N bond length of 1.291 (5) Å is clearly a carbon–nitrogen double bond, and there is no indication of any C=N interaction with the cluster. It should be noted that **6** has an aminoalkyne resonance form. The structure of this resonance form can be predicted from known acetylido complexes with an $HRu_3(CO)_9$ core.[5,13] The shift from a $2e^-$ carbenoid σ-bond between C(2) and Ru(3) in **5** to a $2e^-$ π-interaction with the C(1)–C(2) vector in **6** can be clearly seen by superimposing the two structures in profile (Figure 7).

The ^1H NMR spectrum of **6** shows the expected resonances for the hydride at −16.94 (1) ppm and the two nonequivalent isopropyl groups (two septuplets at 4.42 (1) and 3.95 (1) ppm and two doublets 1.41 (6) and 1.39 (6) ppm; J = 6.84 and 6.35 Hz, respectively). The variable-temperature ^{13}C NMR spectrum of a ^{13}CO-enriched sample of **6** showed a low-temperature limiting spectrum at −10 °C consisting of five resonances at 198.3 (1), 197.2 (2), 195.3 (2), 192.6 (2), and 186.9 (2) ppm, consistent with the symmetry of the solid-state structure. As the temperature is

Table VI. Bond Distances and Angles for $(\mu\text{-H})(\mu_3\text{-}\eta^2\text{-CC=N(CH(CH}_3)_2)_2)\text{Ru}_3(\text{CO})_9$ (6)[a]

	Distances, Å		
Ru1–Ru2	2.7807 (4)	O22–C22	1.133 (5)
Ru2–Ru2′	2.8578 (4)		
Ru1–C1	2.241 (4)	N–C2	1.291 (5)
Ru1–C2	2.121 (4)	N–C3	1.484 (6)
Ru1–C11	1.920 (5)	N–C5	1.528 (7)
Ru1–C12	1.911 (4)	C1–C2	1.341 (6)
Ru2–C1	2.030 (3)	O23–C23	1.128 (5)
Ru2–C21	1.941 (4)	O12–C12	1.136 (5)
Ru2–C23	1.896 (4)	C11–O11	1.126 (6)
Ru2–C22	1.914 (4)	C3–C4	1.535 (6)
O21–C21	1.115 (5)	C5–C6	1.546 (7)
	Angles, deg		
Ru2–Ru1–C1	46.17 (8)	C21–Ru2–C22	96.8 (2)
Ru2–Ru1–C2	74.5 (1)	C23–Ru2–C22	95.1 (2)
Ru2–Ru1–C11	87.4 (1)	C2–N–C3	121.8 (4)
Ru2–Ru1–C12	99.4 (1)	C2–N–C5	119.8 (4)
C1–Ru1–C2	35.7 (2)	C3–N–C5	118.4 (4)
C1–Ru1–C11	123.2 (2)	Ru1–C1–Ru2	81.1 (1)
C1–Ru1–C12	117.9 (1)	Ru1–C1–C2	67.3 (3)
C2–Ru1–C11	158.9 (2)	Ru2–C1–C2	125.4 (2)
C2–Ru1–C12	96.6 (1)	Ru1–C2–N	140.7 (4)
C11–Ru1–C12	97.1 (2)	Ru1–C2–C1	77.0 (3)
Ru1–Ru2–C1	52.8 (1)	N–C2–C1	142.2 (5)
Ru1–Ru2–C21	100.3 (1)	Ru2–C21–O21	178.3 (3)
Ru1–Ru2–C23	90.9 (1)	Ru2–C23–O23	177.2 (4)
Ru1–Ru2–C22	161.2 (1)	Ru2–C22–O22	179.5 (3)
C1–Ru2–C21	151.3 (2)	Ru1–C11–O11	180 (0)
C1–Ru2–C23	94.7 (1)	Ru1–C12–O12	178.1 (3)
C1–Ru2–C22	108.9 (2)	N–C3–C4	108.8 (3)
C21–Ru2–C23	95.6 (2)	N–C5–C6	109.3 (3)

[a] Numbers in parentheses are estimated standard deviations in the least significant digits.

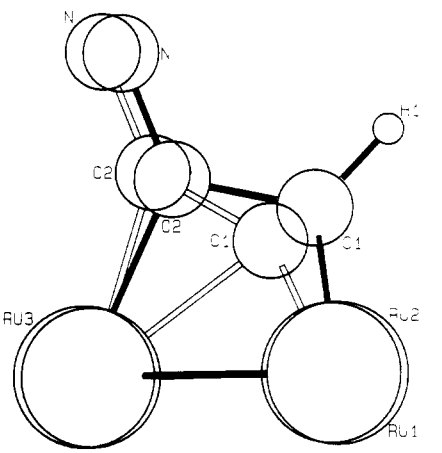

Figure 7. Superposition of the metal core and organic ligand in **5** and **6** illustrating the change in the interaction at Ru(3) from σ-C(2) to π-C(1)–C(2).

(11) Adams, R. D.; Tanner, J. T. *Organometallics* **1988**, *7*, 2241.
(12) Shapley, J. R.; Tachikawa, M.; Churchill, M. R.; Lashewycz, R. A. *J. Organomet. Chem.* **1978**, *162*, C39.
(13) Catti, M.; Gervasio, G.; Mason, S. A. *J. Chem. Soc., Dalton Trans.* **1977**, 2260.
(14) Rosenberg, E.; Milone, L.; Aime, S.; Osella, D.; Gobetto, R. *Organometallics* **1982**, *1*, 640.

increased to +23 °C, the resonances at 198.3 and 192.6 ppm begin to broaden and coalesce, indicating axial–radial exchange at Ru(1). These data are entirely analogous with other $HRu_3(CO)_9$ (5e⁻-donor ligand) systems where the capping organic ligand is rigid.[5,13]

It appeared to us that complexes **5** and **6** could be related to each other by the reductive elimination of H_2 from **5** coupled with C–H oxidative addition. Indeed when **5** is heated in heptane for 1.5 h under N_2 almost quantitative conversion to **6** is observed (eq 3). The reverse process

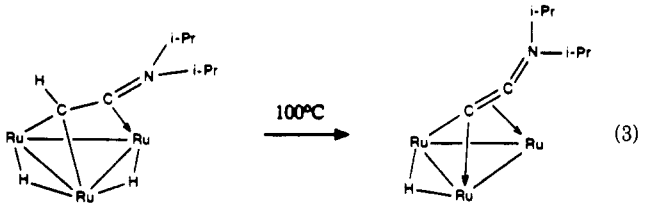

5 6 (3)

however does not proceed cleanly, with decomposition of **6** occurring in the presence of H_2 at 100 °C, presumably by further reduction of the organic ligand.

It should be mentioned that in addition to **5** and **6** a third product is isolated in 10% yield. This compound proved to be $(\mu\text{-H})Ru_3(CO)_{10}(\mu\text{-P}(C_6H_5)_2)$ on the basis of infrared, mass, and ^1H NMR spectral analysis. Significant amounts of the monosubstituted phosphine derivative $Fe_2(CO)_5(P(C_6H_5)_3)(\mu\text{-}SCH_2CH_3)_2$ are also formed. It has not been determined whether direct phosphine transfer from the iron dimer to $Ru_3(CO)_{12}$ or phosphine dissociation followed by substitution on ruthenium is responsible for the formation of this product.

Mechanistic Considerations. The suggested mechanism by which complexes of the type $Fe_2(CO)_4(P(C_6H_5)_3)_2(\mu\text{-}SCH_2CH_3)_2$ promote substitution reactions in clusters has been discussed and to some degree tested elsewhere.[15] Although it is premature at this point to try to propose a detailed mechanism for the formation of complexes **1–6** from tertiary amines and $Ru_3(CO)_{12}$, we think there are some reasonably sound mechanistic constructs that can be put forward at this point in our investigations. The compounds **1–4** resulting from the reaction of triethylamine with $Ru_3(CO)_{12}$ can be divided into two groups: (1) two isomeric compounds from which an alkyl group has been eliminated and (2) two isomeric compounds in which a C_2 fragment has been coupled to the elements of triethylamine. Within each pair the isomers differ in what appears to be α,α-activation versus α,β-activation of the C–H bonds of an ethyl group. If one assumes that, as with C–C activation, C–N activation is preceded by C–H activation and that C–N cleavage proceeds through a carbene–amine complex as previously proposed by Laine,[2] one can generate a schematic representation for the formation of **1–4** (Schemes III and IV). After carbene–amine formation, dissociation of the carbene (presumably followed by dimerization to an alkene) moeity from the cluster could lead directly to **1** and **2** as shown in Scheme III, via subsequent N–H and then two α or one α and one β C–H oxidative additions to the cluster. On the other hand, amine dissociation could be followed by coordination of a second molecule of triethylamine, which could lead to the formation of **3** and **4** as shown in Scheme IV. Of course, carbene dissociation from the cluster followed by attack of the carbene on a Ru_3–amine complex is also possible but less likely in view of the tendency for free carbenes to dimerize. An intermolecular carbene transfer between two clusters is yet a third but less likely possibility. We have ruled out the possibility that **3** and **4** form from **1** by showing that **1** is unreactive toward triethylamine in refluxing hexane in the presence or absence of the iron dimer catalyst.

The most stable isomer resulting from initial coordination of the amine probably has the amine in the radial position as has been shown for bulky ligands such as phosphines in osmium and ruthenium clusters.[16] We propose that in order to enter the carbon–nitrogen bond cleavage manifold shown in Schemes III and IV, migration to an axial position is required. For the case of osmium carbonyl clusters reacting with triethylamine, radial to axial migration is a much higher energy process than in ruthenium,[17] and this results in the edge-bridged product initially formed with no carbon–nitrogen bond cleavage (eq 2), which subsequently forms the direct analogue of **5**. In the case of ruthenium carbonyl reacting with the bulky ethyldiisopropylamine, radial to axial migration would be expected to be much slower than in the case of triethylamine, and so the radially coordinated amine enters the reaction manifold shown in eq 2, resulting in the formation of **5** which then goes on to form **6**. This interpretation of our results is further supported by the recent report of a stable edge-bridged amino alkyne complex $Os_3(CO)_{10}(\mu\text{-}CH_3C_2N(CH_3)_2)$[18] and by our recent results that showed a direct dependence of edge-to-face migration rates on the products formed from the reaction of $H_2Os_3(CO)_{10}$ with terminal alkynes.[19]

The mechanistic proposals presented in Schemes III and IV are currently being investigated by utilizing cyclic amines where early intermediates might be stabilized by a chelation effect and by examination of the reaction volatiles for the presence of secondary amines and dimerized carbenes. We are also exploring the specific role of the iron catalyst used here in the formation of **1–6** by examining the reaction of tertiary amines with $Ru_3(CO)_{12}$ in the presence of sodium benzophenone ketyl or trimethylamine *N*-oxide and with $Ru_3(CO)_{10}(CH_3CN)_2$.

One can conclude from these results that for nitrogen-containing compounds of comparable basicity the facile cleavage of carbon–nitrogen bonds is very sensitive to the steric bulk of the amine. However, it would be premature to extend this trend to understanding the hydrodenitrification process since the results obtained here could be peculiar to the steric requirements of trinuclear clusters.

Experimental Section

Materials. $Ru_3(CO)_{12}$ was purchased from Strem Chemicals. The catalyst $Fe_2(CO)_4(P(C_6H_5)_3)_2(\mu\text{-}SCH_2CH_3)_2$ was synthesized from $Fe_3(CO)_{12}$ (Strem) by known procedures.[20] Triethylamine and ethyldiisopropylamine were purchased from Aldrich and used as received. All solvents were degassed with N_2 and dried over molecular sieves before use.

Spectra. ^1H and ^{13}C NMR spectra were obtained on a JEOL GX 270/89 spectrometer. Infrared spectra were obtained on a Perkin-Elmer 580B spectrometer. Mass spectra were obtained by the U.C. Riverside NSF-Regional Facility using fast atom bombardment methods. Elemental analyses were performed by

(15) Aime, S.; Botta, M.; Gobetto, R.; Osella, D. *Organometallics* **1985**, *4*, 1425.

(16) (a) Churchill, M. R.; DeBoer, B. G. *Inorg. Chem.* **1976**, *16*, 2397. (b) Rosenberg, E.; Skinner, D.; Aime, S.; Milone, L.; Sappa, E. *Inorg. Chem.* **1980**, *19*, 1571.

(17) Rosenberg, E.; Milone, L.; Aime, S. *Inorg. Chim. Acta* **1975**, *15*, 53.

(18) Adams, R. D.; Tanner, J. T. *Organometallics* **1989**, *8*, 563.

(19) Rosenberg, E.; Anslyn, E. V.; Milone, L.; Aime, S.; Gobetto, R.; Osella, D. *Gazz. Chim. Ital.* **1988**, *118*, 299.

(20) Kettle, S.; Orgel, L. E. *J. Chem. Soc., Dalton Trans.* **1960**, 3890.

Scheme III. Possible Mechanism for Formation of 1 and 2

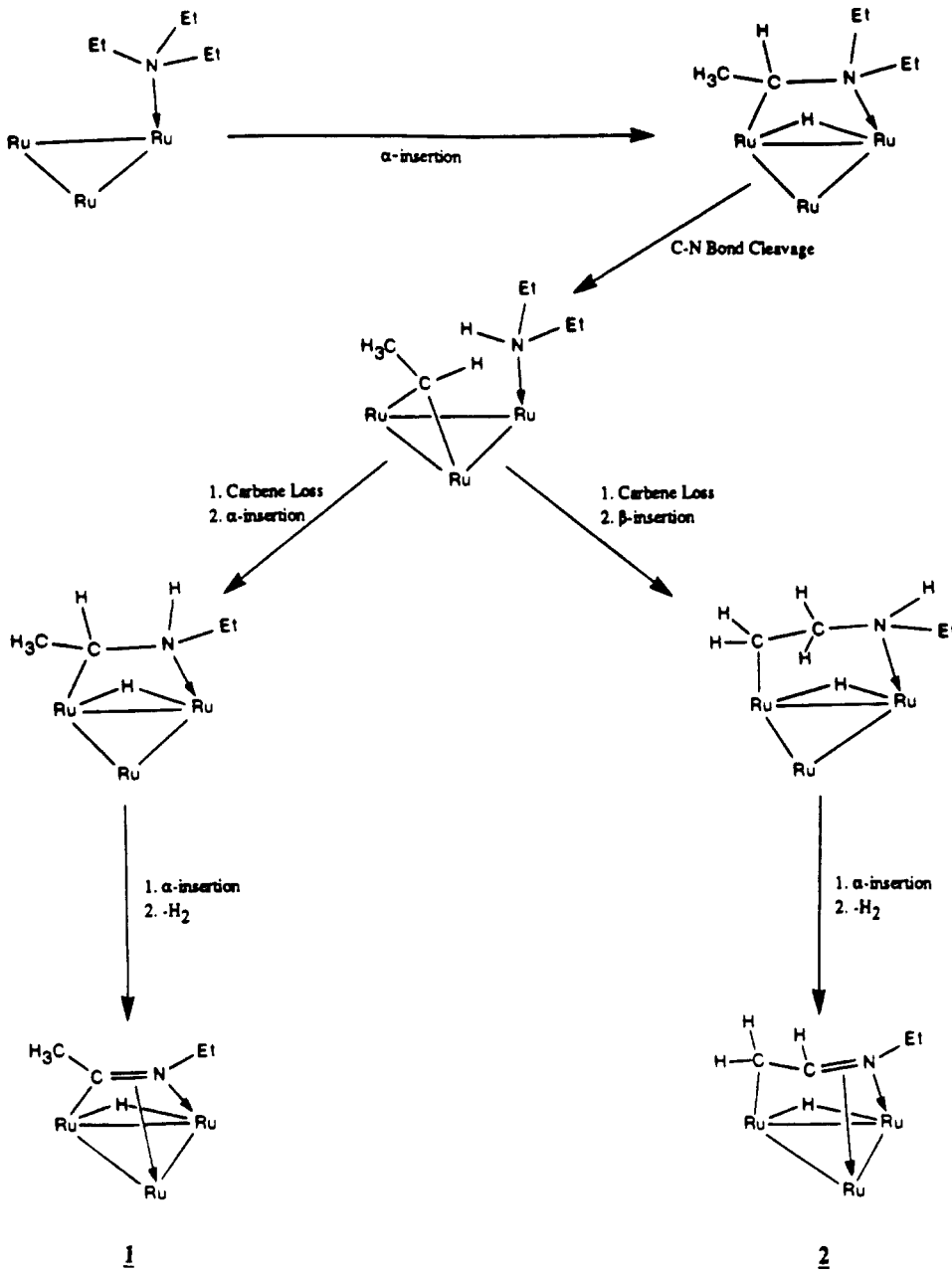

1 2

Schwartzkopf Analytical Laboratories, New York, NY.

Synthesis of Compounds 1–4. In a three-neck flask were combined 300 mg (0.45 mmol) of $Ru_3(CO)_{12}$, 50 mg (0.057 mmol) of $Fe_2(CO)_4(P(C_6H_5)_3)_2(\mu\text{-}SCH_2CH_3)_2$, 2.0 mL (14.34 mmoles) of triethylamine, and 250 mL of hexanes. The solution was refluxed under nitrogen for 6 h and then filtered, and the solvent removed under vacuum. The residue was taken up in methylene chloride and eluted on four 20 × 20 cm silica gel TLC plates with hexanes. This procedure resolved three yellow bands on the upper half of the plates which were $Ru_3(CO)_{12}$ (50 mg), **2** (5–10 mg, ~5% based on consumed $Ru_3(CO)_{12}$), and 1 30 mg (25%). The lower half of the plate showed several partially resolved bands that were isolated as one and rechromatographed by using 20% diethyl ether and 80% hexanes and gave four major bands, which were $Fe_2(CO)_5(P(C_6H_5)_3)(\mu\text{-}SCH_2CH_3)_2$ (10 mg), $Fe_2(CO)_4(P(C_6H_5)_3)_2(\mu\text{-}SCH_2CH_3)_2$ (10 mg), **3** (10 mg, 5%), and **4**, respectively. The iron complexes were identified by their infrared spectra. Compound **4** required a third chromatography using 10% diethyl ether and 90% hexane to obtain analytically pure material (15–20 mg, ~10%).

Analytical Data. Compound **1**: see ref 1. Compound **2**: Anal. Calc for $C_{13}H_9NO_9Ru_3$: 24.92, C; 1.43, H. Found: 24.73, C; 1.58, H. Infrared (cyclohexane) ν(CO) 2091 (m), 2064 (s), 2036 (vs), 2020 (s), 2010 (m), 2002 (m), 1996 (m), 1977 (br) cm^{-1}; mass spec M^+ = 626, calc 626.4. Compound **3**: Anal. Calc for $C_{17}H_{15}NO_9Ru_3$: 30.00, C; 2.22, H. Found: 30.23, C; 2.31 H. IR (*n*-hexane) ν(CO) 2085 (s), 2056 (s), 2029 (vs), 2014 (s), 1999 (m), 1995 (m, br), 1972 (br). Compound **4**: Anal. Calc for $C_{17}H_{15}NO_9Ru_3$: 30.00, C; 2.22, H. Found: 30.15, C: 2.12, H. Infrared (cyclohexane) ν(CO) 2080 (s), 2052 (s), 2048 (s), 2024 (vs), 2006 (s), 1998 (s, br), 1972 (s, br) cm^{-1}; mass spec M^+ = 681, calc 680.5; ^{13}C NMR (–65 °C, $CDCl_3$, ^{13}CO region, intensity 1 if not otherwise stated) 206.41, 204.90, 200.80 (^2J = 11 Hz), 200.14, 199.57, 198.87, 198.72 (2), 198.58, 196.38, 196.68 (^2J = 14.4 Hz), 194.38, 193.37, 193.21, 192.16 (^2J = 13.2 Hz), 191.67, 190.24, 188.49 ppm.

Synthesis of Compounds 5 and 6. In a three-neck round-bottom flask were combined 300 mg (0.45 mmol) of $Ru_3(CO)_{12}$, 50 mg (0.057 mmol) of $Fe_2(CO)_4(P(C_6H_5)_3)_2(\mu\text{-}SCH_2CH_3)_2$, 2.0 mL (11.48 mmol) of ethyldiisopropylamine, and 250 mL of cyclohexane. The mixture was refluxed under N_2 for 12 h, filtered, rotary evaporated, taken up in methylene chloride, and then eluted with hexanes on four 20 × 40 cm silica gel TLC plates to resolve five bands. The first band contained unreacted $Ru_3(CO)_{12}$ and compound **5**, the second contained mostly compound **6** and minor impurities, the third contained pure $(\mu\text{-}H)(\mu\text{-}P(C_6H_5)_2)Ru_3(CO)_{10}$, and the fourth and fifth were $Fe_2(CO)_5P(C_6H_5)_3(\mu\text{-}SCH_2CH_3)_2$

Scheme IV. Possible Mechanism for Formation of 3 and 4

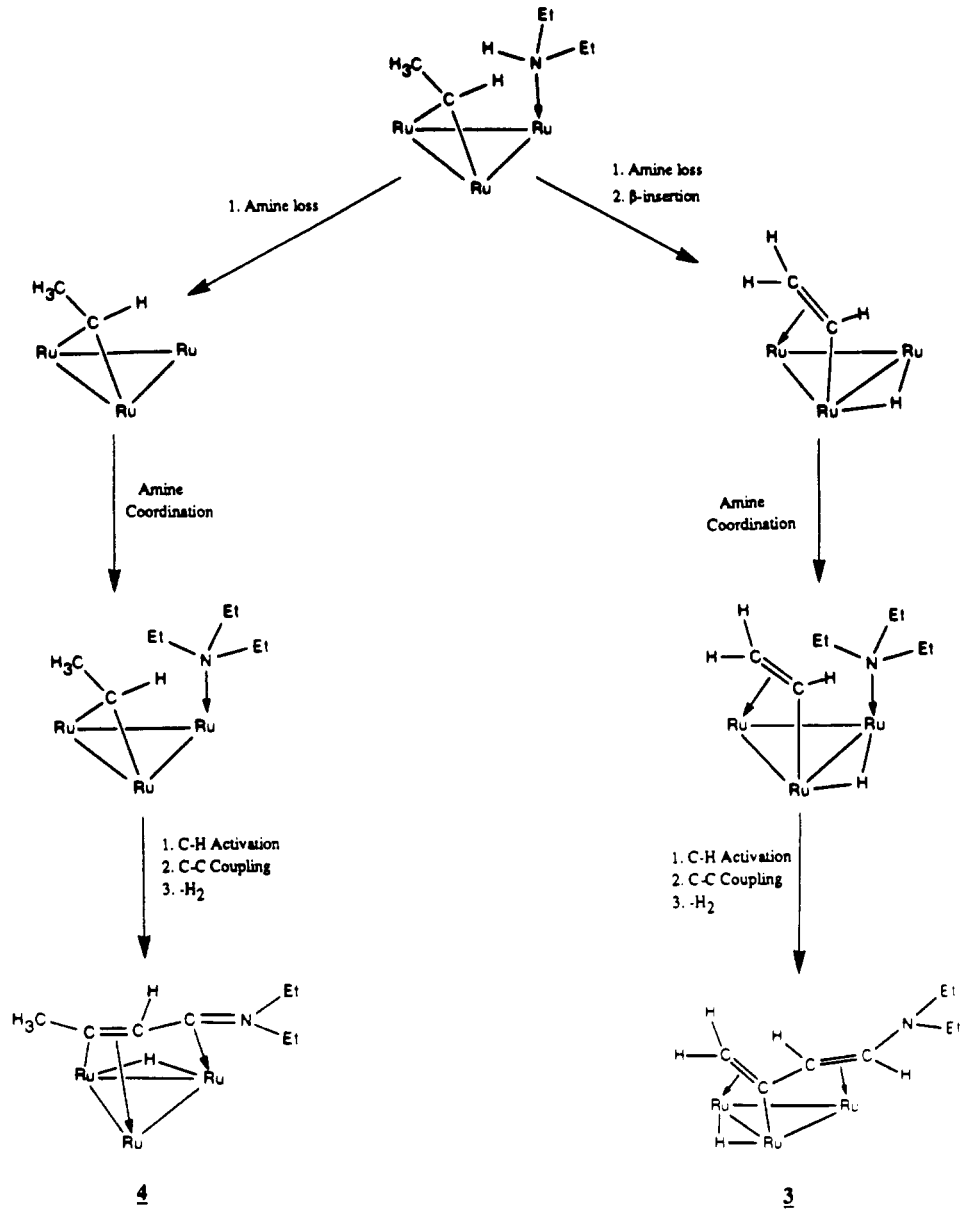

and $Fe_2(CO)_4(P(C_6H_5)_3)_2(\mu\text{-}SCH_2CH_3)_2$, respectively. Band one was reeluted on silica gel TLC plates with hexanes to yield two bands, which were identified as $Ru_3(CO)_{12}$ and compound **5** (30–40 mg, ~15%). Band two was reeluted with hexanes on silica gel to yield one major band containing compound **6** (20–30 mg, ~ 10%).

Analytical Data. Compound **5**: Anal. Calc for $C_{17}H_{17}NO_9Ru_3$: 29.91, C; 2.51, H. Found: 29.86, C; 2.18, H. IR (*n*-hexane) ν(CO) 2096 (m), 2066 (s), 2042 (vs), 2028 (m), 2020 (m), 2002 (m), 1987 (m, br), 1969 (br) cm^{-1}; mass spec M^+ = 654, calc 654.47. Compound **6**: Anal. Calc for $C_{17}H_{15}NO_9Ru_3$: 30.05, C; 2.22, H. Found: 29.85, C; 2.02, H. IR (*n*-hexane) ν(CO) 2082 (m), 2055 (s), 2031 (s), 1992 (br), 1966 (w), 1945 (w) cm^{-1}; mass spec M^+ = 652, calc 652.3. $(\mu\text{-}H)(\mu\text{-}P(C_6H_5)_2)Ru_3(CO)_{10}$: Anal. Calc for $C_{22}H_{11}O_{10}PRu_3$: 27.6, C; 1.70, H. Found: 27.42, C; 1.92, H. IR (cyclohexane) ν(CO) 2095 (w), 2045 (w), 2024 (m), 2015 (vs), 1986 (w) cm^{-1}; ^1H NMR (acetone-d_6) δ 7.54 m (10), −17.18 (d, J(PH) = 3.6 Hz (1)).

Conversion of 5 to 6. Compound **5** (50 mg, 0.07 mmole) in 50 mL of *n*-heptane was refluxed under nitrogen for 1.5 h, at which time the infrared spectrum indicated complete conversion to **6**. The solution was rotary evaporated, and the residue taken up in methylene chloride and chromatographed on silica gel by using 5% diethyl ether and 95% hexanes. Only one major band was eluted, which proved to be **6** by infrared and ^1H NMR spectroscopies; yield 40–45 mg (80–90%).

X-ray Structure Determination of 3. A yellow crystal of compound **3** obtained by recrystallization from hexane at −20 °C and measuring 0.15 × 0.45 × 0.40 mm^3 was used to obtain unit-cell constants and intensity data. Fifteen intense reflections were selected in the range $11.0° < 2\theta < 27.0°$ from rotation photographs about the φ-axis on a four-circle Siemens (Nicolet) $P2_1$ diffractometer using monochromic Mo Kα radiation. Refined unit cell parameters and orientation matrix for data collection were determined from 15 accurately centered reflections in the range $14.0° < 2\theta < 32.0°$ using the centering and least-squares programs of the $P2_1$ system. Photographs taken along the refined cell axis confirmed triclinic symmetry of the crystal. Further details of data collection and reduction have been published previously.[1] A summary of crystal data and data collection parameters appears in Table I.

The structure was solved by direct methods using MULTAN.[21] The coordinates of the ruthenium atoms obtained from the E-map were used for phasing the trial structure and calculating structure factors and a Fourier difference map. All non-hydrogen atoms in the structure were located in additional structure factor–difference Fourier cycles. The structure was refined by using a

(21) MULTAN: A system of computer programs for the automatic solution of crystal structures from X-ray diffraction data: Germain, G.; Main, P.; Woolfson, M. M. *Acta Crystallogr., Sect. A.: Cryst. Phys. Diffr., Theor. Gen. Crystallogr.* **1971**, *A27*, 368.

full-matrix least-squares technique. During refinement the function minimized was $\sum w(|F_o| - |F_c|)^2$, where the weights were defined by $w = 1/\sigma^2(F_o)$. All non-hydrogen atoms were refined with anisotropic thermal parameters. At this point structure factors and difference Fourier synthesis revealed the location of most of the hydrogen atoms in the structure. The remaining hydrogen atoms were input at calculated positions for a final cycle of refinement of all non-hydrogen atoms. Agreement factors and residual electron density in the final structure are collected in Table I. Neutral atomic scattering factors were used for all atoms, and anomalous dispersion corrections for Ru atoms were included in the refinement and structure factor calculations.

X-ray Structure Determination of 4–6. Crystals of **4** were obtained by slow evaporation of a saturated hexane solution at room temperature; crystals of **5** and **6** were obtained by recrystallization from saturated hexane solutions cooled to −20 °C. Suitable crystals having approximate dimensions of 0.25 × 0.25 × 0.25 mm^3 for **4**, 0.54 × 0.14 × 0.13 mm^3 for **5**, and 0.30 × 0.38 × 0.33 mm^3 for **6** were each mounted on glass fibers, placed in a goniometer head on an Enraf-Nonius CAD4 diffractometer, and centered optically. Unit cell parameters and an orientation matrix for data collection were obtained from 21 reflections with $22° < 2\theta < 35°$ for **4**, 25 reflections with $12° < 2\theta < 30°$ for **5**, and 25 reflections with $14° < 2\theta < 34°$ for **6**, using the centering program in the CAD4 system. Details of the crystal data are given in Table I. Systematic absences $h0l$, $l = 2n + 1$, $0k0$, $k = 2n + 1$ for **4** indicate the monoclinic space group $P2_1/c$, systematic absences $h00$, $h = 2n + 1$, $0k0$, $k = 2n + 1$, $00l$, $l = 2n + 1$ for **5** indicate the orthorhombic space group $P2_12_12_1$, and systematic absences $0kl$, $k + l = 2n + 1$ and $hk0$, $h = 2n + 1$ indicated the orthorhombic space group *Pnma* for **6**. These were verified by successful least-squares refinement of the structure. Data were collected at room temperature by using the ω scan technique to a maximum 2θ angle of 58° for **4**, 67° for **5**, and 68° for **6**. For each crystal the actual scan range was calculated by scan width = 0.8 + 0.35 tan θ, and background intensities were measured by using the moving-crystal stationary-counter technique at the beginning and end of each scan. As a check on crystal and electronic stability, three representative reflections were measured every 2 h. Lorentz and polarization and decay corrections were applied to the data, as was an empirical absorption correction based on a series of ψ scans. A total of 6415 reflections were measured for **4** of which 4585 with $F_o \geq 3\sigma(F_o)$ were employed, a total of 5071 reflections were measured for **5** of which 3706 having $F_o \geq 3\sigma(F_o)$ were employed, and a total of 5288 reflections were measured for **6** of which 3224 having $F_o \geq 3\sigma(F_o)$ were used. All other reflections were considered to be unobserved.

Structures of **4–6** were solved by standard Patterson methods, which revealed the positions of the metal atoms. All other non-hydrogen atoms were found by successive difference Fourier synthesis.[22] The hydridic hydrogen atomic positions were calculated by using HYDEX,[7] and the positions of the vinylidenic hydrogens on C(1), the hydrogens on C(3) and C(4) in compound **4**, and the hydrogen attached to C(1) in compound **5** were calculated by using HYDRO.[23] These positioned hydrogen atoms were included but not refined in the final least-squares cycles; all non-hydrogen atoms were refined anisotropically. Due to apparent disorder of C(6) in compound **4** this atom was forced to refine as a riding atom on C(5). Selected bond distances are in Table IV–VII, and the residual electron density in the final structures are listed in Table I.

Scattering factors were taken from Cromer and Waber.[24] Anomalous dispersion corrections were those of Cromer.[25] All calculations were carried out on a DEC MicroVaxII computer using the SDP/VAX system of programs.[23]

Acknowledgment. We gratefully acknowledge the National Science Foundation for support (CHE8711549) and for a diffractometer grant, the NATO Science Program (R.G. 0705/87; E.R. and L.M.), the donors of the Petroleum Research Foundation, administered by the American Chemical Society (PRF 19781B3C), and Coniglio Nazionale delle Ricerche for support of this research.

Supplementary Material Available: Atomic positions for **3–6** (Tables VII–X) and anisotropic displacement factors (Tables XI–XIV) (16 pages); observed and calculated structure factors (Tables XV–XVIII) (135 pages). Ordering information is given on any current masthead page.

(22) Sheldrick, G. M. SHELXS-86, Program for Crystal Structure Solution, University of Gottingen, 1986.

(23) HYDRO: Frenz, B. A. The Enraf-Nonius CAD 4 SDP—A Real-time System for Concurrent X-Ray Data Collection and Crystal Structure Determination. In *Computing in Crystallography*; Schenk, H., Olthof-hazelkamp, R., vonKonigsveld, H., Bassi, G. CCc., Eds.; Delft University Press: Delft, Holland, 1978; pp 64–71.

(24) Cromer, D. T.; Waber, J. T. *International Tables of X-ray Crystallography*; The Kynoch Press: Birmingham, England, 1974; Vol. IV, Table 2.2B.

(25) Cromer, D. T. *International Tables for X-ray Crystallography*; The Kynoch Press: Birmingham, England, 1974; Vol. IV, Table 2.3.1.